

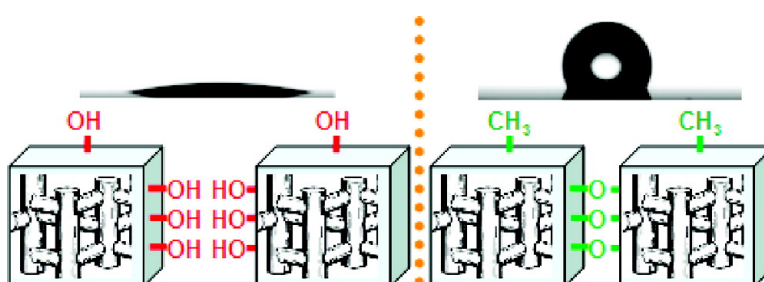
Communication

Ultraviolet-Assisted Curing of Polycrystalline Pure-Silica Zeolites: Hydrophobization, Functionalization, and Cross-Linking of Grains

Salvador Eslava, Francesca Iacopi, Mikhail R. Baklanov,
 Christine E. A. Kirschhock, Karen Maex, and Johan A. Martens

J. Am. Chem. Soc., **2007**, 129 (30), 9288-9289 • DOI: 10.1021/ja0723737 • Publication Date (Web): 11 July 2007

Downloaded from <http://pubs.acs.org> on February 16, 2009



More About This Article

Additional resources and features associated with this article are available within the HTML version:

- Supporting Information
- Links to the 10 articles that cite this article, as of the time of this article download
- Access to high resolution figures
- Links to articles and content related to this article
- Copyright permission to reproduce figures and/or text from this article

[View the Full Text HTML](#)



ACS Publications
 High quality. High impact.

Ultraviolet-Assisted Curing of Polycrystalline Pure-Silica Zeolites: Hydrophobization, Functionalization, and Cross-Linking of Grains

Salvador Eslava,^{*,†,‡} Francesca Iacopi,[†] Mikhail R. Baklanov,[†] Christine E. A. Kirschhock,[§] Karen Maex,^{†,‡} and Johan A. Martens[§]

Interuniversity MicroElectronic Center (IMEC), Kapeldreef 75, 3001 Leuven, Belgium, Centrum voor Oppervlaktechemie en Katalyse, Katholieke Universiteit Leuven, Kasteelpark Arenberg 23, 3001 Leuven, Belgium, and Department of Electrical Engineering (ESAT-INSYS), Katholieke Universiteit Leuven, Kasteelpark Arenberg 10, 3001 Leuven, Belgium

Received April 4, 2007; E-mail: eslava@imec.be

Zeolite and zeolite-like films attract the attention of many research groups due to their applications in separation processes,¹ chemical syntheses,² sensors,³ and integrated circuits.⁴ A variety of pure-silica zeolites, such as Silicalite-1,^{4,5} Silicalite-2,⁶ and pure-silica BETA,⁷ have been grown as polycrystalline films on porous and nonporous supports. The applicability of these films strongly depends on their hydrophobicity and porosity, both compromised by the presence of grain boundaries. One example is the application of Silicalite-1 in integrated circuits as an ultralow dielectric constant material (ultralow *k*). A suitable deposition method is the spin-on deposition of Silicalite-1 suspensions containing Silicalite-1 nanocrystals and primary silica nanoparticles⁸ of ~4 nm.⁴ Despite the hydrophobicity of the Silicalite-1 micropores, the polycrystalline film is hydrophilic due to the presence of external silanols, which hampers the application. To address this issue, a vapor-phase treatment, such as a silylation, can be applied.⁴ However, a treatment with a reactive vapor has limitations due to pore blocking in micropores.^{9,10} An alternative is the addition of methyltrimethoxysilane to the zeolite synthesis to incorporate hydrophobic methyl groups. However, when such film is heated above 355 °C to remove the organic template, the gain of hydrophobicity is decreased.^{4c}

Research in porous organo-silica glasses reveals that the combination of ultraviolet irradiation and thermal activation, termed UV-assisted curing, effectively generates a favorable rearrangement in the chemical bond structure.¹¹ In this work, we demonstrate the advantageous use of a UV-assisted curing for the hydrophobization of polycrystalline zeolites. A spin-on Silicalite-1 film serves as an example. The UV-assisted curing hydrophobizes the porous structure by both silanol condensation and grafting of desorbing organic template fragments. Moreover, it facilitates the packing of the grains, so the intergrain voids are substantially decreased and the mechanical properties improved.

Spin-on Silicalite-1 films were prepared from a Silicalite-1 suspension synthesized with tetrapropylammonium (TPA) as organic template following the recipe of Wang et al.⁴ An as-deposited film was UV-assisted cured for 5 min by heating in an inert atmosphere at 425 °C and simultaneously exposing it to a high-intensity broadband UV radiation roughly in the 200–400 nm range. For comparison, another film was calcined in air at the same temperature.

IR spectra of as-deposited, calcined, and UV-assisted cured Silicalite-1 films are shown in Figure 1. The as-deposited film shows intense IR absorptions assigned to the TPA template molecules (2860–3000, 1475 and 1370 cm⁻¹). The IR bands due to TPA

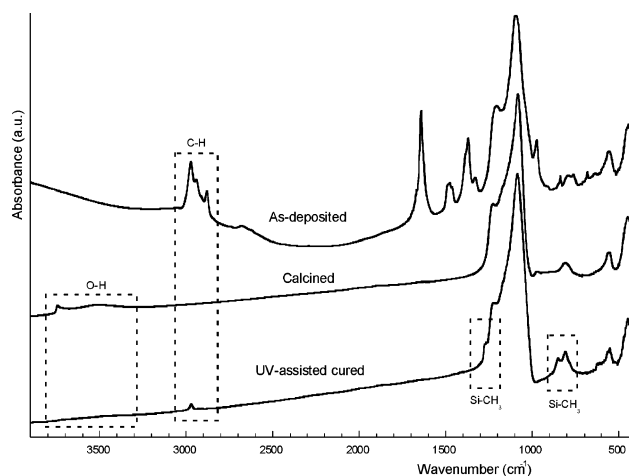


Figure 1. FTIR absorbance of spin-on Silicalite-1 films in the IR region of 3900–400 cm⁻¹.

disappear upon calcination and UV-assisted curing. In the UV-assisted cured film, weaker IR absorption remains at 2860–3000 cm⁻¹ (C–H stretching) and new IR absorption bands appear that are assigned to methyl groups bonded to silicon atoms as Si–(CH₃)_x, 1 ≤ *x* ≤ 3 (1260–1280 and 800–900 cm⁻¹).¹² Therefore, the UV-assisted curing not only evacuates effectively the TPA template but also makes fragments of TPA molecules react with the silicate matrix leading to methylation. The combination of UV irradiation and heating is essential for obtaining the grafting of organic template fragments. Without heating, merely photochemical decomposition and desorption of the organic template have been reported for UV-irradiated organic-templated silica films.¹³ The calcined film contains silanol groups: 3745 cm⁻¹ (isolated silanols); 3450–3700 cm⁻¹ (H-bonded silanols and water); and 980 cm⁻¹ (Si–OH). In contrast to calcination, the UV-assisted curing leads to a drastic reduction of silanol vibration bands. Moreover, the UV-assisted curing, in comparison to calcination, leads to a higher increase in the internal asymmetric stretching (1110–1070 cm⁻¹) relative to the external asymmetric stretching (1220 cm⁻¹) of the Si–O–Si bond. This increase has been reported to be linked to the cross-linking and fusion of silicate particles.⁸ Both effects on the silanol vibration and the Si–O–Si stretching reveal that UV-assisted curing enhances the cross-linking and fusion of the grains in this polycrystalline Silicalite-1 film. Thus, the Silicalite-1 structure contains a minimal number of active sites for water uptake.

The contact angles of water on the top surface of the films increases from 10(±5)° in calcined film to 137(±11)° in the UV-assisted cured film. For comparison, the hydrophobization approach via addition of methyltrimethoxysilane in the zeolite synthesis

[†] IMEC.

[‡] ESAT-INSYS.

[§] Centrum voor Oppervlaktechemie en Katalyse.

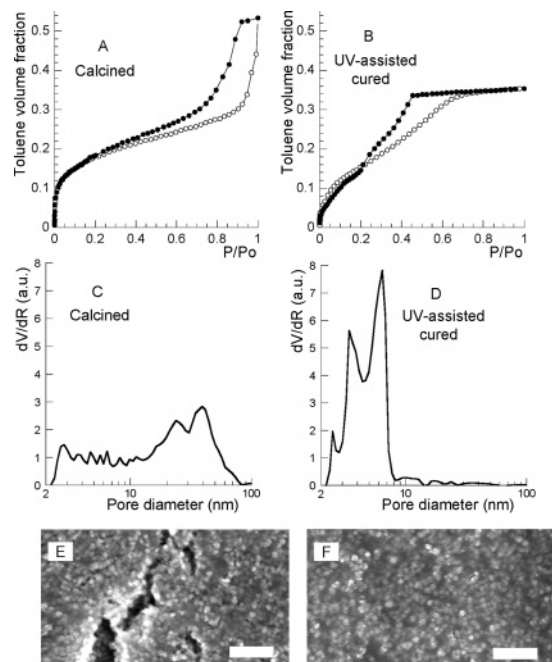


Figure 2. Toluene adsorption isotherms in spin-on Silicalite-1 film that was calcined (A) and UV-assisted cured (B). (○) Adsorption, (●) desorption. Pore size distribution in calcined film (C) and UV-assisted cured film (D) from 2 nm. SEM images of spin-on Silicalite-1 films that were calcined (E) and UV-assisted cured (F). Scale bar = 500 nm.

resulted in a contact angle of ca. 45° .^{4c} Water adsorption isotherms of the films determined by ellipsometric porosimetry¹⁴ confirm that the internal volume also becomes very hydrophobic upon UV-assisted curing, as adsorbed water decreases from 34 to 5% (See Supporting Information, Figure S1). This significant difference in hydrophobicity–hydrophilicity is in agreement with the observations in FTIR spectroscopy (Figure 1), that is, with the low content of silanols and the organic functionalization of the film upon UV-assisted curing. The hydrophobicity substantially meliorates the application of spin-on Silicalite-1 films in integrated circuits. UV-assisted cured Silicalite-1 film has an ultralow dielectric constant of $2.16(\pm 0.02)$, which only increases 5% in humid ambient. In calcined film, the increase is $\sim 300\%$ (Supporting Information, Figure S2).

Panels A and B in Figure 2 show toluene adsorption isotherms on calcined and UV-assisted cured films, respectively, measured by ellipsometric porosimetry.¹⁵ The toluene adsorption isotherms present significant hysteresis which is due to capillary condensation in intergrain voids. The total porosity of the film derived from the maximum toluene uptake is 35 and 53 vol % for UV-assisted cured and calcined films, respectively. The toluene relative pressure needed for saturating the UV-assisted cured film is significantly lower than that for calcined film, indicating that intergrain voids are shrunk. The mesopore size distribution shows that voids in the UV-assisted cured film measure from 2 to 8 nm, whereas in the calcined film, they extend up to values higher than 50 nm (panels C and D in Figure 2). This shrinking is a result of the unique cross-linking and fusion obtained by UV-assisted curing.

The quality of pure-silica zeolite films is linked with its crystallinity,^{4b,16} but at high crystallinity, the removal of the organic template by calcination often leads to formation of cracks.¹⁷ Inspection using scanning electron microscopy (SEM) taught us that spin-on Silicalite-1 films with a nanocrystal content higher than 30 wt % (on silicon basis) always show cracks after calcination. Films with a nanocrystal content higher than 50 wt % frequently

delaminate upon calcination. Figure 2 shows SEM images of the Silicalite-1 films discussed in this paper with a nanocrystal content of 63 wt %. Cracks are present in the calcined film, and delamination is often encountered, whereas the same film subjected to UV-assisted curing apparently has no cracks according to SEM and does not delaminate. Then, the UV-assisted curing offers a means to substantially improve the mechanical quality of high-nanocrystal-content films. Actually, nanoindentation determines that the elastic modulus and hardness are $10.7(\pm 3.2)$ and $1.1(\pm 0.4)$ GPa for UV-assisted cured Silicalite-1 film and $6.2(\pm 1.5)$ and $0.5(\pm 0.2)$ GPa for the calcined Silicalite-1 film. This difference is attributed to the enhanced effects of the UV-assisted curing on the cross-linking of the silicate grains.

The synthesis of Silicalite-1 films by using the UV-assisted curing was repeated several times showing reproducible Si–CH₃ content, hydrophobicity, and mechanical properties.

In conclusion, we have demonstrated that UV-assisted curing hydrophobizes spin-on Silicalite-1 films by means of silanol condensation and organic functionalization. The latter is uniquely achieved by the grafting of the organic template. Moreover, the silanol condensation enhances the fusion of the grains, minimizing the intergrain drawbacks. This has beneficial effects on the mechanical properties and pore size distribution. The success of the UV-assisted curing on spin-on Silicalite-1 films will inspire new avenues in modification of zeolite-like materials, supported or unsupported.

Acknowledgment. The authors acknowledge C. Waldfried and O. Escorcía for the UV-assisted curing performed in Axcelis, MA. C.E.A.K. and J.A.M. acknowledge the Flemish government for a concerted research action (GOA).

Supporting Information Available: Experimental procedure and Figures S1 and S2. This material is available free of charge via the Internet at <http://pubs.acs.org>.

References

- (1) Coronas, J.; Santamaria, J. *Sep. Purif. Methods* **1999**, *28*, 127–177.
- (2) Saracco, G.; Specchia, V. *Catal. Rev.-Sci Eng.* **1994**, *36*, 305–384.
- (3) Yan, Y. A.; Bein, T. *J. Am. Chem. Soc.* **1995**, *117*, 9990–9994.
- (4) (a) Wang, Z. B.; Mitra, A. P.; Wang, H. T.; Huang, L. M.; Yan, Y. S. *Adv. Mater.* **2001**, *13*, 1463–1466. (b) Li, Z.; Li, S.; Luo, H.; Yan, Y. S. *Adv. Funct. Mater.* **2004**, *14*, 1019–1024. (c) Li, S.; Li, Z.; Medina, D.; Lew, C.; Yan, Y. S. *Chem. Mater.* **2005**, *17*, 1851–1854.
- (5) Wang, Z. B.; Yan, Y. S. *Chem. Mater.* **2001**, *13*, 1101–1107.
- (6) Dong, J.; Xu, Y.; Long, Y. *Microporous Mesoporous Mater.* **2005**, *87*, 59–66.
- (7) Mintova, S.; Reinelt, M.; Metzger, T. H.; Senker, J.; Bein, T. *Chem. Commun.* **2003**, *3*, 326–327.
- (8) Kirschhock, C. E. A.; Ravishanker, R.; Verpeurt, F.; Grobet, P. J.; Jacobs, P. A.; Martens, J. A. *J. Phys. Chem. B* **1999**, *103*, 4965–4971.
- (9) O'Connor, C. T.; Möller, K. P.; Manstein, H. *J. Mol. Catal. A: Chem.* **2002**, *181*, 15–24.
- (10) Impens, N. R. E. N.; van der Voort, P.; Vansant, E. F. *Microporous Mesoporous Mater.* **1999**, *28*, 217–232.
- (11) (a) Iacopi, F.; Travaly, Y.; Eyckens, B.; Waldfried, C.; Abell, T.; Guyer, E. P.; Gage, D. M.; Dauskardt, R. H.; Sajavaara, T.; Houthoofd, K.; Grobet, P.; Jacobs, P.; Maex, K. *J. Appl. Phys.* **2006**, *99*, 053511. (b) Iacopi, F.; Beyer, G.; Travaly, Y.; Waldfried, C.; Gage, D. M.; Dauskardt, R. H.; Houthoofd, K.; Jacobs, P.; Adriaens, P.; Schulze, K.; Schulz, S. E.; List, S.; Carloti, G. *Acta Mater.* **2007**, *55*, 1407–1414.
- (12) Grill, A.; Neumayer, D. A. *J. Appl. Phys.* **2003**, *94*, 6697–6707.
- (13) Dattelbaum, A. M.; Amweg, M. L.; Ruiz, J. D.; Ecke, L. E.; Shreve, A. P.; Parikh, A. N. *J. Phys. Chem. B* **2005**, *109*, 14551–14556.
- (14) Baklanov, M. R.; Mogilnikov, K. P.; Le, Q. T. *Microelectron. Eng.* **2006**, *83*, 2287–2291.
- (15) Baklanov, M. R.; Mogilnikov, K. P.; Polovinkin, V. G.; Dultsev, F. N. *J. Vac. Sci. Technol. B* **2000**, *18*, 1385–1391.
- (16) Eslava-Fernandez, S.; Baklanov, M. R.; Iacopi, F.; Brongersma, S. H.; Kirschhock, C. E. A.; Maex, K. *Mater. Res. Soc. Symp. Proc.* **2006**, *914*, 0914-F03-08.
- (17) Geus, E. R.; van Bekkum, H. *Zeolites* **1995**, *15*, 333–341.

JA0723737